Postharvest Biology and Technology 230 (2025) 113787

Contents lists available at ScienceDirect

Postharvest Biology and Technology

journal homepage: www.elsevier.com/locate/postharvbio

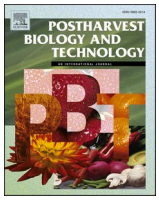

Harvest maturity modulates the synchronization between exocarp color change and mesocarp softening in avocado cv. Hass: A multiomics perspective

Camila Arancibia-Guerra [a], Gerardo Núñez-Lillo [a], Ignacia Hernández [b], Excequel Ponce [a], Nathalie Kuhn [a], Alegría Carrasco-Pancorbo [c], Lucía Olmo-García [c], Esther Carrera [d], Jorge Baños [d], David Campos [e], Bruno Defilippi [f], Reinaldo Campos-Vargas [g], Claudio Meneses [h,i,j], Romina Pedreschi [a,j,*]

[a] Escuela de Agronomía, Facultad de Ciencias Agronómicas y de los Alimentos, Pontificia Universidad Católica de Valparaíso, Quillota, Chile
[b] Departamento de Producción Vegetal, Facultad de Agronomía, Universidad de Concepción, Concepción, Chile
[c] Department of Analytical Chemistry, Faculty of Sciences, University of Granada, Granada, Spain
[d] Instituto de Biología Molecular y Celular de Plantas, Universidad Politécnica de Valencia-Consejo Superior de Investigaciones Científicas, Valencia, Spain
[e] Universidad Nacional Agraria La Molina, Instituto de Biotecnología, Lima, Peru
[f] Instituto de Investigaciones Agropecuarias (INIA-La Platina), Santiago, Chile
[g] Centro de Estudios Postcosecha, Facultad de Ciencias Agronómicas, Universidad de Chile, Santiago 8831314, Chile
[h] Departamento de Fruticultura y Enología, Facultad de Agronomía y Sistemas Naturales, Pontificia Universidad Católica de Chile, Santiago, Chile
[i] Facultad de Ciencias Biológicas, Pontificia Universidad Católica de Chile, Santiago, Chile
[j] Millennium Institute Center for Genome Regulation (CRG), Santiago, Chile

ARTICLE INFO

Keywords:
Color development
Physiological disorder
Persea americana
Anthocyanins
Omics

ABSTRACT

Avocado cv. Hass is a crop of worldwide importance and demand. Fruit mesocarp firmness and exocarp color are essential parameters determining Hass avocado ripening and consumer acceptability. Exocarp color de-synchronization with softening is a relevant recurrent problem for the avocado supply chain, particularly during marketing. This research aimed to investigate how harvest maturity influences this quality issue by metabolomic, transcriptomic, and hormonal differences in avocado fruit collected at different harvest maturities. In addition, early potential biomarkers of exocarp color – mesocarp firmness de-synchronized fruit at harvest are proposed. Integration of multi-omics data revealed an overactivation of the phenylpropanoid pathway in early harvested fruits, particularly at key branches associated with the biosynthesis of lignin, quercetin, and epicatechins derivatives-metabolic processes that are linked to a higher incidence of color-softening desynchronization. In contrast, late harvest fruits, less susceptible to this disorder, exhibited enhanced expression of genes involved in the anthocyanin biosynthesis pathway compared to early harvest samples. We propose quinic acid, β-sitosterol, mannoheptulose as early harvest biomarkers and indole acetic acid (IAA), xylitol and arabitol for late harvest biomarkers. These findings suggest that in late harvest fruits, the colour transition process is already underway at time of harvest, promoting a more synchronized progression between exocarp coloration and mesocarp softening.

1. Introduction

Avocado consumption has increased worldwide due to its nutritional benefits (e.g., mono and polyunsaturated fatty acids, vitamins, fiber, etc.). Hass is the most widely marketed avocado variety worldwide, including in Chile, with a production of 155.000 t during the 2023/2024 season, where 70 % of production was destined for export to Europe and United States (Comité de Palta Hass Chile, 2024).

The physiology of avocado is very peculiar in terms of extended flowering period, low fruit set, and inability to ripen on the tree. These

* Corresponding author at: Escuela de Agronomía, Facultad de Ciencias Agronómicas y de los Alimentos, Pontificia Universidad Católica de Valparaíso, Quillota, Chile.
E-mail address: romina.pedreschi@pucv.cl (R. Pedreschi).

https://doi.org/10.1016/j.postharvbio.2025.113787
Received 23 May 2025; Received in revised form 15 July 2025; Accepted 16 July 2025
Available online 22 July 2025

traits contribute to significant fruit heterogeneity within a tree and harvest batches, which only becomes evident during postharvest management and marketing (Hernández et al., 2016). Fruit mesocarp firmness and exocarp color are essential parameters that determine 'Hass' avocado ripening and consumer acceptability (Hernández et al., 2016). After harvest, as the fruit ripens, firmness decreases significantly (from values as high as 140 N to 4–14 N), while the exocarp color transitions from green to black (Cox et al., 2004; Ashton et al., 2006). The synchronization of ripening in terms of mesocarp softening and exocarp color change is crucial for the marketing of fruit as ready to eat (Olmedo et al., 2024). In recent seasons, problems of ripening heterogeneity and desynchronization between exocarp color and mesocarp softening have been reported by different producing and importing countries (Mathaba et al., 2015, 2016, 2017; Mathe et al., 2018; Arancibia-Guerra et al., 2022), leading consumers to make wrong decisions generating logistic problems and increasing food losses, which have been reported as high as 10–30 % (Landahl and Terry, 2020).

This exocarp-mesocarp ripening desynchronization involves changes in the content of main pigments present in the exocarp (chlorophylls, carotenoids, and anthocyanins), which are known to be regulated by a complex hormonal interplay, with ethylene, abscisic acid, and cytokinins playing central roles (Arancibia-Guerra et al., 2022; Núñez-Lillo et al., 2023; Olmedo et al., 2024). For instance, unsynchronized, known as "green fruit", is characterized by a lower production of anthocyanins, specifically, cyanidin-3-*O*-glucoside, the main anthocyanin in the exocarp of 'Hass' avocado, responsible for the purplish/black tones (Cox et al., 2004; Arancibia-Guerra et al., 2022). Different pre-harvest factors, including climatic variables and harvest maturity, have been previously reported to affect the color development of 'Hass' avocado exocarp at the ready-to-eat stage (Rivera et al., 2017; Mathaba et al., 2016; Mathaba et al., 2017).

Commercial harvest of avocado is based on a minimum dry matter content that depends on oil content that varies among different countries and legislations for avocado cultivars. For instance, the Chilean Hass avocado Committee has established a minimum dry matter (DM) mesocarp content of 23 % (~9 % oil content) for exports. Other countries, such as Peru, have established a minimum of 21.5 % DM, while the EU has established a minimum of 21 % DM for 'Hass' (EU Regulation N°387/2005). Previous studies have reported that the mesocarp DM content at harvest is not a reliable indicator of physiological age or subsequent ripening behavior in avocados (Rivera et al., 2017; Pedreschi et al., 2014; Hernández et al., 2021). Additionally, other studies have shown that early harvest 'Hass' avocados (with low DM content) exhibited the greatest issues with synchronization between exocarp color and mesocarp firmness at the ready-to-eat stage (Arancibia-Guerra et al., 2022; Mathe et al., 2018); however, the underlying causes remain unclear.

We hypothesize that exocarp color and mesocarp softening desynchronization in 'Hass' avocado is mainly influenced by harvest maturity, and to a less extent to seasonal climatic factors, which induce differential transcriptomic, metabolic, and hormonal responses in the fruit exocarp. These differential responses result in distinctive biochemical signatures at harvest, serving as potential biomarkers to predict the desynchronization disorder at the ready-to-eat stage. Thus, the aim of this study is: (i) to phenotype the exocarp color-mesocarp softening desynchronization problem in a large amount of 'Hass' avocado batches from different agroclimatic zones, harvest dates and harvest seasons; (ii) to integrate omics data (transcriptomics and metabolomics) and hormones from avocado exocarp of different harvest maturity in a selected orchard displaying differences in color phenotype at the ready-to-eat stage and (iii) to select potential at harvest biomarkers for this problem.

2. Materials and methods

2.1. Fruit material and storage conditions

One thousand two hundred avocado fruits cv. 'Hass' per orchard were sampled across three harvest maturity stages (detailed below) during the 2022/2023 and 2023/2024 seasons. Orchards were located in different agroclimatic zones (interior, intermediate, and coastal). The agroclimatic zones have the following characteristics: a) interior zone: distance from orchard to sea were between 300 and 900 m above sea level; b) intermediate zone: distance from orchard to sea of 20 and 45 km and elevation from 300 to 400 m above sea level; c) coastal zone: distance from orchard to sea $\leq$ 10 km and elevation between 100 and 250 m above sea level.

Sampling considered three different maturities at harvest according to dry matter content (DM): early (18–23 % DM), middle (>23–27 % DM), and late (>27–30 % DM) (Table S1). From each orchard and harvest maturity, one hundred fruits were stored under regular air (RA; at 5 °C for 30 days) and the remaining 100 fruits in controlled atmosphere conditions (CA, at 5 °C and 4 kPa CO_2 and 6 kPa O_2). After storage, the fruit was brought to shelf-life at 20 °C until each fruit reached the ready-to-eat stage (RTE) (4–14 N). Firmness of each fruit was measured non-destructively at harvest, during RA storage, and during shelf-life storage with a texture analyzer (TAXT Plus, Stable Micro System, Godalming, UK).

Exocarp tissue from 10 independent fruits from each orchard at harvest was frozen, ground in liquid nitrogen immediately after sampling and stored at −80 °C until analysis. A total of 5 biological replicates composed of two fruit each were obtained for further analysis. Based on the results of the assessment of color desynchronization with softening (Section 3.1) at RTE, samples from different harvest times (early, middle, and late) and two complete seasons were further analyzed to assess the effect of harvest maturity on this disorder using an omics integration approach as detailed below.

2.2. Assessment of color desynchronization with softening

2.2.1. Skin color

Skin color was measured on each fruit individually with a colorimeter (CR-400 Minolta) at harvest and at the RTE stage. Four color measurements were carried out in the equatorial zone of each fruit, using CIELab color coordinates, where L* is lightness, a* and b* represent the red-green and yellow-blue axes, C* (chroma) represents the intensity/purity of color, and h° is the hue angle on the color wheel. The exocarp coloration at the ready-to-eat (RTE) stage was quantified using the hedonic color scale established by Ferreyra and Defilippi (2012), which assigns discrete categorical score as follow: (1) emerald green, (2) forest green, (3) olive green, (4) purple, and (5) black. According to this scale, scores of 1 through 3 are categorized as 'green-stage' fruit, while scores of 4 and 5 denote 'black-stage' fruit.

2.2.2. Targeted pigment analysis

Total chlorophyll, carotenoid, and anthocyanin extractions were carried out using 30 mg of dry exocarp as reported by Lichtenthaler and Buschmann (2001) with some modifications, using ethanol as extracting agent. Chlorophylls and carotenoids were determined by measuring the absorbance at 470, 648, 664, and 750 nm, and the final contents were calculated following the equations:

$$Chlorophyll\ A = (13.36 \times Abs_{664}) - (5.19 \times Abs_{648})$$

$$Chlorophyll\ B = (27.43 \times Abs_{648}) - (8.12 \times Abs_{664})$$

$$Carotenoids = \frac{(1000 \times Abs_{470}) - (2.13 \times Chla) - (97.64 \times Chlb)}{209}$$

Anthocyanins were measured by the pH differential method as

described in Giusti and Wrolstad (2001) at absorbances of 520 and 700 nm, respectively. Anthocyanins were expressed as cyanidin 3-*O*-glucoside equivalents:

$$Total\ anthocyanins = \frac{Abs\ total \times MW \times Fd \times 1000}{\varepsilon}$$

Where Abs total = $(Abs_{520} - Abs_{700})\ pH_{1.0} - (Abs_{520} - Abs_{700})\ pH_{4.5}$; MW = 449.2 g mol^{-1}; Fd = dilution factor; ε = 26900, molecular extinction coefficient.

Formula concentration was expressed in mg g^{-1} and it was corrected considering the concentration of the samples (g mL^{-1} for chlorophyll and carotenoids and g L^{-1} for anthocyanin). The final concentration of different pigments was expressed as mg pigment kg^{-1} DM exocarp tissue.

2.3. Determination of total phenolic compounds

The extracts were obtained using the methodology reported by Saavedra et al. (2017). Fifty mg of freeze-dried avocado exocarp was mixed with 2 mL of acetone. The mixture was shaken for 1.0 h and centrifuged at 13,500 rpm for 20 min at 4 °C. Total phenolic content (TPC) was determined using the Folin-Ciocalteau method. Sample absorbance was measured at 765 nm, and values were expressed as g of gallic acid equivalents (GAE) kg^{-1} of dry weight (DW).

2.4. HPLC-PDA phenolic compounds profile

Phenolic extracts were obtained as described by Núñez-Lillo et al. (2024) using methanol. Phenolic compounds were analyzed using a high-performance liquid chromatography with a quaternary pump (PU-4180) system equipped with a photodiode array detector (PDA, MD-4010) and an autosampler AS-4050 (JASCO, Tokyo, Japan). The column used for separation was ZORBAX Eclipse Plus C_{18} (150 mm × 4.6 mm, 1.8 μm; Agilent Technologies, Santa Clara, CA, USA). The mobile phase comprised solvent A (0.5 % acetic acid in water) and solvent B (acetonitrile). The gradient ran as follows: 1 min, 90 % A; 7 min, 85 % A; 19 min, 75 % A; 20 min, 70 % A; 25 min, 30 % A; 40 min, 30 % A; 41 min, 90 % A; 50 min, 90 % A. The flow rate was kept constant at 0.35 mL min^{-1}, and an injection volume of 5 μL was used. The phenolic compounds were detected and identified by comparing their retention time and ultraviolet-visible (UV-Vis) spectral data with known standards previously injected (at 280, 320, and 370 nm). The results were expressed in g compound kg^{-1} DW.

For the anthocyanin profile, 50 mg of freeze-dried sample was subjected to a methanol extraction. The column used for separation was Kromasil 100 C_{18} (250 mm × 4.6 mm, 5 μm; Sigma-Aldrich, St. Louis, MO, USA). The mobile phase consisted of solvent A (5 % acetic acid in water) and solvent B (acetonitrile with 0.1 % acetic acid). The gradient was as follows: 1 min, 7 % B; 25 min, 12 % B; 26 min, 95 % B; 30 min, 95 % B; 31 min, 5 % B; 35 min, 5 % B. The flow rate was 0.8 mL min^{-1}, and an injection volume of 10 μL was used. Anthocyanins were detected and identified by comparing retention time and UV-Vis spectral data at 520 nm.

2.5. GC-MS polar metabolite analysis

The extraction and derivatization of polar metabolites were carried out following the protocol described by Hatoum et al. (2014), with adaptations as specified by Fuentealba et al. (2017). In summary, 25 mg of freeze-dried exocarp tissue was subjected to methanol-based extraction, followed by sequential derivatization steps consisting of methoximation and trimethylsilylation. Metabolite profiling was performed using an Agilent 7890B gas chromatograph coupled to a PAL3 autosampler and a 5977 A single quadrupole mass spectrometer with an electron impact ionization source (EI 350). Separation was achieved using an HP-5-MS Ultra Inert capillary column (30 m × 0.25 mm, 0.25 μm; Agilent Technologies, Santa Clara, CA, USA). The analysis focused on key primary metabolites, specifically targeting sugars, amino acids, and organic acids. For high abundance compounds such as sugars, a 1:50 split injection was employed with the oven program initiated at 120 °C for 1 min, ramped to 300 °C at 10 °C min^{-1}, and held for 6 min. In contrast, for lower abundance analytes such as organic and amino acids, a splitless injection mode was applied with an oven temperature starting at 50 °C for 1 min, increasing to 310 °C at 10 °C min^{-1}, and held for 13 min. The injector and interface temperatures were maintained at 220 °C and 280 °C, respectively. One μL of each sample was injected, and helium served as the carrier gas at a constant flow rate of 1 mL min^{-1}. Ion source and quadrupole temperatures were set at 230 °C and 150 °C, respectively. Mass spectra were acquired at a scanning speed of 2.66 scans s^{-1} within the m/z range of 50–600. Metabolite identification was based on retention time and mass spectral data, using a custom-built library of commercial standards and the NIST14 database, processed through MassHunter Quantitative software (Agilent Technologies, Santa Clara, CA, USA). Results were expressed as relative metabolite abundances.

Differential abundance analysis of metabolomic data was performed using MetaboAnalyst software v6.0. The data were subsequently scaled using the auto-scaling method (mean-centered and divided by the standard deviation of each variable). Differentially abundant metabolites (DAM) between the studied conditions were determined with a one-way ANOVA test using a false discovery rate (FDR) cutoff of 0.05. Finally, any metabolite that did not exhibit a monotonic ascending or descending abundance across the early, middle, and late conditions was subsequently removed from the dataset.

2.6. Transcriptomic analysis

2.6.1. RNA extraction and library construction

Total RNA was isolated from 100 mg of frozen exocarp tissue using the Spectrum™ Plant Total RNA Kit (Sigma-Aldrich, St. Louis, Missouri, USA), following the manufacturer's protocol, and subsequently stored at –80 °C. RNA concentration and purity were assessed using a Qubit® 2.0 fluorometer (Invitrogen™, Carlsbad, California, USA) with the Qubit™ RNA BR and RNA IQ assay kits. RNA integrity was determined by the RNA Quality Number (RQN), and only samples with RQN values exceeding eight were selected for library preparation. Libraries were constructed using the TruSeq Stranded Total RNA Kit (Illumina, San Diego, CA, USA), in accordance with the manufacturer's recommendations. The concentration of the libraries was quantified with a Qubit® 4.0 fluorometer (Invitrogen™) using the Qubit™ dsDNA BR assay kit, while library fragment size and integrity were evaluated via capillary electrophoresis using the Automated CE Fragment Analyzer™ system (Agilent Technologies, Santa Clara, CA, USA) and the DNF-474–0500 HS NGS Fragment Kit. A total of 15 libraries (representing 3 conditions with 5 biological replicates each) were sequenced by BMK Technologies (Beijing, China) using an Illumina NovaSeqX platform in paired-end mode, with a read length of 150 bp.

2.6.2. Differential expression analysis

Quality assessment of raw sequencing reads was carried out using FASTQC software, followed by preprocessing with Flexbar v3.5.0 (Dobd et al., 2012) under the following criteria: (i) removal of adapter sequences, (ii) exclusion of reads with Phred quality scores below 30, and (iii) filtering out reads shorter than 60 base pairs. The filtered reads were aligned to the *Persea americana* var. Drymifolia´ reference genome v3.0 using the STAR aligner v2.7.10 (Dobin et al., 2013). Gene expression quantification was performed using the featureCounts function from the R package Rsubread v2.8.1 (Liao et al., 2019), considering only uniquely mapped fragments.

Differential gene expression analysis was conducted with the edgeR package v3.36.0 (Robinson et al., 2010), using trimmed mean of

M-values (TMM) normalization. Genes were considered differentially expressed (DEGs) if they met the criteria of $|\log_2$ fold change$| > 0.5$ and a false discovery rate (FDR) < 0.05. Multivariate discrimination was explored through partial least squares discriminant analysis (PLS-DA) using the plsda and plotIndiv functions in the mixOmics package v6.20.0 (Rohart et al., 2017). Additionally, a heatmap of monotonic DEGs was generated using the pheatmap package v1.0.12. Functional enrichment analysis of DEGs was conducted using the gene ontology (GO) database with the ClusterProfiler package v4.0.5 (Yu et al., 2012), applying the compareCluster function to identify significantly enriched biological processes and pathways.

2.7. Hormone analysis

Fifteen exocarp samples of avocado were collected at harvest during two consecutive seasons (2022/2023 and 2023/2024) for hormonal analysis. Quantification of abscisic acid (ABA), jasmonic acid (JA), salicylic acid (SA), indole-3-acetic acid (IAA), several gibberellins (GA_1, GA_4, GA_8, GA_{12}, GA_{20}, and GA_{24}), and cytokinins (trans-zeatin [tZ], isopentenyladenine [iP], and dihydrozeatin [DHZ]) was conducted following an extraction protocol adapted from Seo et al. (2011). Samples were suspended in 80 % methanol containing 1 % acetic acid and internal standards and homogenized by shaking for 1 h at 4 °C. Extracts were stored overnight at –20 °C, centrifuged, and the resulting supernatants were concentrated to dryness under vacuum. The resulting residues were reconstituted in 1 % acetic acid and subjected to solid-phase extraction using reverse-phase HLB Oasis cartridges (30 mg; Waters Corporation, Milford, MA, USA), followed by purification through Oasis MCX (cation exchange) columns (Waters Corporation, Milford, MA, USA). Cytokinins were isolated as the basic fraction, eluted with 60 % methanol containing 5 % ammonium hydroxide from the MCX column. Acidic hormones (ABA, JA, SA, IAA, and GAs) were recovered with 100 % methanol containing 1 % acetic acid. For samples requiring enhanced resolution, an additional purification step using Oasis WAX ion-exchange columns (Waters Corporation, Milford, MA, USA) eluted with 80 % methanol–1 % acetic acid was performed. Final residues were dissolved in 5 % acetonitrile–1 % acetic acid prior to chromatographic analysis. Hormonal separation was carried out via Ultra High-Performance Liquid Chromatography using a reverse-phase Accucore C_{18} column (100 mm, 2.6 μm; Thermo Fisher Scientific, Waltham, MA, USA), with a 0.05 % acetic acid acetonitrile gradient at a flow rate of 0.4 mL min^{-1} . The acetonitrile gradient ranged from 2 % to 55 % over 21 min for acidic hormones and from 2 % to 25 % over 13 min for cytokinins. Detection was performed using a Q-Exactive Orbitrap mass spectrometer (Thermo Fisher Scientific, San Diego, CA, USA) in targeted Selected Ion Monitoring (tSIM) mode. Electrospray ionization (ESI) was applied in negative mode for acidic hormones and in positive mode for cytokinins. Operating conditions included a capillary temperature of 300 °C, spray voltage of 3.0 kV, heater temperature of 150 °C, S-lens RF level of 70, resolution of 70,000, sheath gas flow at 40 μL min^{-1} , and auxiliary gas flow at 10 μL min^{-1} . Hormone concentrations were expressed as μg H kg^{-1} DW, where H denotes hormone content.

2.8. Data analysis and integration

A two-way analysis of variance (ANOVA) was performed to evaluate the effects and interaction between harvest maturity and season in orchards from different agroclimatic zones using a $p < 0.05$, followed by a Tukey test using R software version 4.0.2 (Vienna, Austria) with significance set at $p < 0.05$. Differences in metabolites and hormones at harvest were assessed by one-way ANOVA using a $p < 0.05$. Multi-omics integration for biomarkers of Hass´ avocado exocarp color-mesocarp firmness desynchronization was performed with a MixOmics derived software called DIABLO (Data integration analysis for biomarker discovery using latent components; Singh et al., 2019). To evaluate the number of components to retain in the sparse PLS-DA analysis, a repeated k- fold cross-validation through the DIABLO *perf* function and *the tune.block.splsd* function was used to determine the optimal number of variables of each component. Finally, for variable selection and biomarkers identification, the sparse partial least squares (*s*PLS) analysis was performed. This method was designed to perform simultaneous variable selection during the dimension reduction process to identify a subset of highly correlated or discriminant variables from each omics dataset that contribute most to the shared information between datasets or to the discrimination of biological conditions.

3. Results

3.1. Evaluation of color desynchronization with softening in orchards from different agroclimatic zones and seasons with different harvest maturity

Color desynchronization was highly influenced by the harvest maturity (harvest date) as shown in Table 1. Six out of the seven evaluated orchards displayed significant differences for harvest maturity ($p < 0.05$) as revealed in most of the cases by two-way ANOVA. Early harvested orchards develop an average color rating of 3.5 on the hedonic scale (olive green) across both seasons, regardless of agroclimatic zone. However, coastal orchards exhibited a lower average value compared to interior and intermediate orchards, respectively (3.5 vs 3.9 and 4.1). In the 2022/2023 season, fruit from middle harvest presented improved color development, with orchards averaging color values of 3.9. This trend was also observed in the 2023/2024 season (average color values increased from 3.6 to 3.8 from early to middle harvest); however, coastal orchards again exhibited poor color development. Late harvest fruit, with DM content above 27 %, mostly displayed improved color development in both seasons (4.1 and 3.9 color values for 2022/2023 and 2023/2024 seasons, respectively). In these cases, the exocarp mostly developed the expected black-violet color in Hass´ avocado except for coastal orchards that maintained the olive-green color.

3.2. Selection and phenotyping of an orchard to comprehensibly study exocarp color desynchronization with mesocarp softening

Among the orchards studied, Ensenada was selected for detailed analysis due to its clear trend in exocarp color development across harvest dates (Table 1). Early harvest fruit reached average hedonic color values of 3.7 and 3.5 for the 2022/2023 and 2023/2024 seasons, respectively; middle harvest avocados reached values of 4.1 and 4.0, and late harvest fruit consistently reached a value of 4.2 in both seasons.

Detailed phenotyping data at harvest and ready-to-eat (RTE) stages for both seasons and the three harvest maturities defined by DM content are displayed in Table 2 and Table 3, respectively. This phenotyping encompassed both subjective colour evaluation (based on a hedonic scale) and objective colorimetric analysis (CIELab), along with quantification of total phenolic compounds and the major pigment classes present in the exocarp, including total anthocyanins, total chlorophylls, and total carotenoids. As expected, DM content increased as harvest advanced, average DM contents of 21.1 % ± 3.3 and 20.1 % ± 1.5, 25.5 % ± 1.9 and 28.7 % ± 2.9, and 28.6 % ± 3.5 and 32.0 % ± 1.7 for early, middle and late harvests of 2022/2023 and 2023/2024 seasons were obtained. In general, DM averages comply with the initially defined ranges, except for the middle and late harvest of the 2023/2024 season, which exceeded the range. Concerning color parameters, L, b*, and C showed significant differences between the various harvests across both seasons, at both the harvest (Table 2) and RTE (Table 3) stages. However, at harvest, total chlorophyll content did not differ significantly among the different harvest maturities within each season, but inter-seasonal differences were observed, with higher levels recorded in the 2022/2023 season. In fact, there was a higher average content in the late harvest (642.4 and 444.4 mg kg^{-1} DW for 2022/2023 and 2023/2024 seasons, respectively) compared to the early harvest (512.6

Table 1
Avocado exocarp color development at the ready to eat stage (4–14 N mesocarp firmness) of orchards from different harvest dates (early: 18–23 % DM; middle: >23–27 % DM; late: >27–30 % DM) and two harvest seasons.

Orchard	Agroclimatic zone	Season 2022/2023			Season 2023/2024		
		Early	Middle	Late	Early	Middle	Late
El Rancho†	Coast	3.2^{a}	3.7^{bc}	3.9^{c}	3.4^{ab}	3.3^{ab}	3.5^{abc}
El Peumo†	Coast	3.2^{ab}	3.8^{de}	4.0^{e}	3.4^{bc}	3.0^{a}	3.5^{cd}
Quilhuica	Intermediate	-	-	-	3.6^{a}	4.1^{b}	3.8^{ab}
4 Palmas†	Intermediate	3.5^{a}	4.4 ^{cd}	4.7^{d}	3.9^{b}	4.4 ^{cd}	4.4^{c}
Ensenada	Interior	3.7^{a}	4.1^{b}	4.2^{b}	3.5^{a}	4.0^{b}	4.2^{b}
Bartolillo	Interior	3.5^{a}	3.5^{a}	4.1^{b}	-	-	-
Los Ángeles	Interior	-	-	-	-	4.2^{a}	4.1^{a}

Values of color development are based on a hedonic scale: (1) emerald green, (2) forest green, (3) olive green, (4) purple, (5) black.
A-two-way ANOVA ($p < 0.05$) with harvest date and season as factors was conducted. Different letters in the same row indicate significant differences between harvest dates (Tukey HSD, $p < 0.05$).
†: Significant differences in factor interaction.

Table 2
Exocarp color parameters of avocado cv. Hass from Ensenada at harvest stage.

Evaluated parameters	Season 2022/2023			Season 2023/2024		
	Early	Middle	Late	Early	Middle	Late
DM mesocarp (%)†	21.1^{a}	25.5^{b}	28.6^{bc}	20.1^{a}	28.7^{b}	32.0^{c}
L†	36.2^{d}	34.5^{c}	32.8^{a}	36.8^{e}	33.8^{b}	33.1^{a}
a*†	–12.3^{a}	–10.0^{b}	–4.8^{d}	–12.0^{a}	–9.3^{c}	–8.7^{c}
b*†	18.3^{e}	14.6^{c}	9.2^{a}	17.1^{d}	13.0^{b}	13.7^{bc}
C†	22.0^{e}	17.8^{c}	10.5^{a}	20.9^{d}	16.0^{b}	16.3^{b}
h†	124.1^{c}	124.7 ^{cd}	113.9^{a}	125.2 ^{cd}	125.5^{d}	121.9^{b}
Hedonic scale	1.0^{a}	1.0^{a}	1.0^{a}	1.0^{a}	1.0^{a}	1.0^{a}
Total phenolic content (g GA eq kg^{-1} DM)†	75.5^{b}	72.5^{b}	54.5^{b}	70.6^{b}	16.2^{a}	68.0^{b}
Anthocyanin (mg kg^{-1} DM)†	0.1^{a}	1.4^{a}	74.7^{b}	0.0^{a}	0.4^{a}	6.5^{a}
Chlorophylls (mg kg^{-1} DM)	512.6^{ab}	635.4^{b}	642.4^{b}	381.5^{a}	457.5^{a}	444.4^{a}
Carotenoids (mg kg^{-1} DM)	103.6^{bc}	128.9 ^{cd}	144.9^{d}	71.9^{a}	86.0^{ab}	93.1^{ab}

The results are expressed as the mean value of 5 avocados (n = 5). A-two-way ANOVA ($p < 0.05$) with harvest date and season as factors was conducted. Different letters in the same row indicate significant differences between harvests dates (Tukey HSD, $p < 0.05$).
Hedonic scale: (1) emerald green, (2) forest green, (3) olive green, (4) purple, (5) black.
†: Significant differences in factor interaction.

Table 3
Exocarp color parameters of avocado cv. Hass from Ensenada at the ready to eat (RTE) stage.

Evaluated parameters	Season 2022/2023			Season 2023/2024		
	Early	Middle	Late	Early	Middle	Late
DM mesocarp (%)†	21.1^{a}	25.5^{b}	28.6^{bc}	20.1^{a}	28.7^{b}	32.0^{c}
L†	27.5^{b}	26.8^{a}	28.3^{c}	28.4^{c}	27.5^{b}	27.0^{a}
a*†	3.3^{c}	2.8^{bc}	1.8^{a}	2.5^{b}	2.0^{a}	3.0^{c}
b*†	4.7^{c}	3.4^{b}	3.0^{ab}	5.4^{d}	4.2^{c}	2.7^{a}
C†	6.0^{d}	4.7^{bc}	3.6^{a}	6.3^{d}	4.8^{c}	4.4^{b}
h†	52.2^{bc}	47.2^{b}	57.3 ^{cd}	62.8^{de}	63.2^{e}	40.9^{a}
Hedonic scale	3.7^{a}	4.1^{b}	4.2^{b}	3.5^{a}	4.0^{b}	4.2^{b}
Total Phenolic Content (g GA eq kg^{-1} DM)†	58.2^{b}	59.1^{b}	49.4^{ab}	40.6^{a}	61.2^{b}	49.8^{ab}
Anthocyanin (mg kg^{-1} DM)	105.1^{a}	153.8^{ab}	230.5^{bc}	152.2^{a}	127.0^{a}	248.6^{c}
Chlorophylls (mg kg^{-1} DM)	367.9^{a}	376.7^{a}	461.8^{b}	392.3^{ab}	405.9^{ab}	430.4^{ab}
Carotenoids (mg kg^{-1} DM)	77.0^{a}	75.1^{a}	86.8^{a}	72.8^{a}	74.6^{a}	79.0^{a}

The results are expressed as the mean value of 20 avocados (n = 20). A-two way ANOVA ($p < 0.05$) with harvest date and season as factors was conducted. Different letters in the same row indicate significant differences between harvests dates (Tukey HSD, $p < 0.05$).
Hedonic scale: (1) emerald green, (2) forest green, (3) olive green, (4) purple, (5) black.
†: Significant differences in factor interaction.

and 381 mg kg^{-1} DW for the same seasons). However, in our results for the 2022/2023 season a clear decrease in chlorophyll content from harvest to RTE stage was observed across all harvest dates: early harvest declined from 512.6 to 367.9 mg kg^{-1} DW, middle harvest from 635.4 to 376.7 mg kg^{-1} DW, and late harvest from 642.4 to 461.8 mg kg^{-1} DW. In contrast, during the season 2023/2024, chlorophyll content remained stable between harvest and RTE stages (early harvest, from 381.5 to 392.3 mg kg^{-1} DW; middle harvest, from 457.5 to 405.9 mg kg^{-1} DW; late harvest, from 444.4 to 430.4 mg kg^{-1} DW). A similar trend was observed for total carotenoid content in both seasons. In the present study, chlorophyll content decreased by approximately 50 % from harvest to RTE during the 2022/2023 season, whereas in the subsequent season, chlorophyll levels remained largely unchanged.

At harvest time, low levels of total anthocyanins were detected in the early (0.1 and 0 mg kg^{-1} DW for 2022/2023 and 2023/2024 season, respectively) and middle harvests (1.4 and 0.4 mg kg^{-1} DW for the same seasons). In contrast, late harvest fruit already presented significantly higher ($p < 0.05$) anthocyanins content at harvest (74.7 and 6.5 mg kg^{-1} DW for 2022/223 and 2023/2024 season, respectively).

At the RTE stage, anthocyanin content increased substantially in both seasons (Table 3). In 2022/2023, total anthocyanins reached 105.1 mg kg^{-1} DW, 153.8 mg kg^{-1} DW, and 230.5 mg kg^{-1} DW for early, middle, and late harvests, respectively. Similarly, in 2023/2024, values were 152.2 mg kg^{-1} DW, 127.0 mg kg^{-1} DW and 231.5 mg kg^{-1} DW, respectively.

3.3. *Integration of omics data to unravel the effect of the harvest maturity on exocarp color and mesocarp firmness synchronization*

3.3.1. *Metabolomic and hormone analysis*

To evaluate sample distribution and replicate dispersion in the two evaluated seasons displaying all identified metabolites, a PLS-DA score plot, displaying all identified metabolites is presented in Figure S1. This plot demonstrates a clear separation of the biological conditions, with this distinction primarily achieved by the variate 1. To identify correlations between different type of metabolites, as shown in Fig. 1, three PLS-DA were performed for color-pigment (Fig. 1A; 22 variables including climatic factors, total pigments and color coordinates), polar metabolite (Fig. 1B; 53 variables including sugars, amino acids, organic acids, etc.), and hormone (Fig. 1C; 13 variables including gibberellins, cytokinins, JA, ABA and SA) datasets. Early, middle, and late harvest conditions could be separated using the x-variate 1 with 56 %, 30 %, and

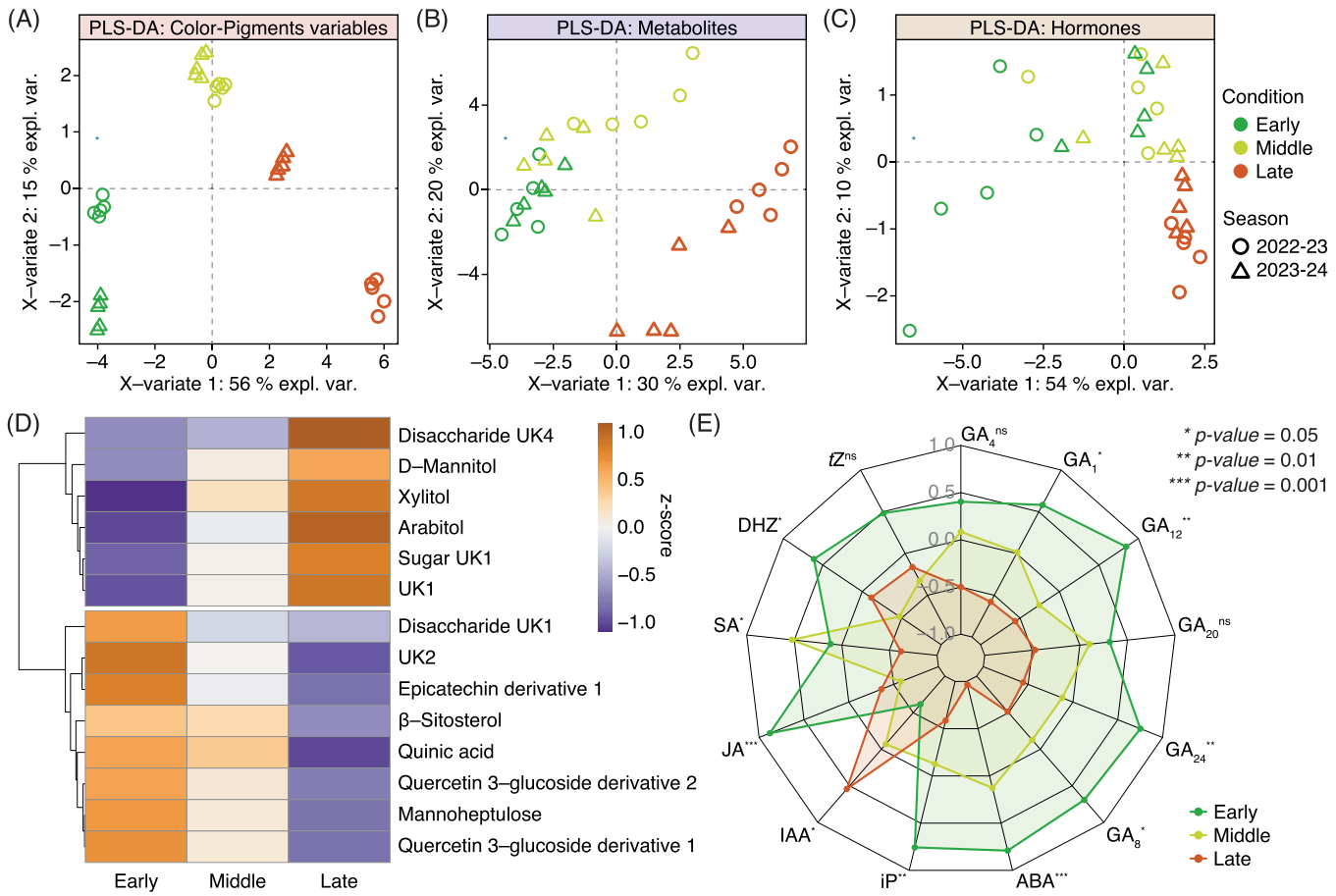

Fig. 1. Comprehensive analysis at harvest of avocado exocarp composition and hormonal profiles across harvests in two evaluated seasons. (A–C) Partial least squares discriminant analysis (PLS-DA) illustrating the distribution of biological replicates across harvests (early, middle and late), based on: (A) colorimetric data (hedonic and CIELAB scales), pigment concentrations (anthocyanins, chlorophylls, phenolics, and carotenoids), and climatic variables; (B) relative abundances of identified polar metabolites; and (C) quantified hormone levels. (D) Heatmap visualizing the z-score transformed relative abundances of all monotonic differentially accumulated metabolites (DAMs) identified across early, middle, and late harvest stages. The color scale represents the magnitude of the z-score, indicating relative enrichment or depletion. Unknown compounds were represented by UK metabolite names. (E) Radar chart depicting the z-score normalized levels of quantified hormones, illustrating changes in hormonal profiles across the different harvest stages. Statistical significance of differences between harvest stages was determined using one-way ANOVA.

54 % explained variance for color-pigment, metabolite, and hormone datasets, respectively. Although the sample distribution differed between the two evaluated seasons, a clear separation between harvest stages was evident in both cases. A color-scaled heatmap was generated using 14 statistically significant metabolites according to an ANOVA test, all of which also exhibited a monotonic metabolite abundance profile (Fig. 1D; Table S2). Among them, 6 metabolites showed higher abundance in late harvest samples, notably D-mannitol, xylitol, and arabitol. The remaining 8 metabolites showed higher abundance in early harvest samples, including mannoheptulose, derivatives of quercetin 3-glucoside and epicatechin, quinic acid, and β-sitosterol.

The targeted hormone analysis is depicted in the radar chart of Fig. 1E. Statistically significant differences in GA_1, GA_8, GA_{12}, GA_{24}, ABA, JA, IAA, SA, DHZ, and iP were observed between early, middle and late harvest conditions. Our results show that GAs, ABA, iP and JA contents were significantly higher in early harvest exocarp compared to later harvests. Consistently, significantly higher IAA levels in late harvest exocarp samples (109.0 μg kg^{-1} DW) compared to middle (84.3 μg kg^{-1} DW) and early harvests (47.4 μg kg^{-1} DW) were identified. On the other hand, SA was more abundant in the middle harvest exocarp samples. Finally, only GAs, ABA, iP, and IAA showed monotonic behavior and correlation with harvest stages.

3.4. Selection of early (at harvest) biomarkers associated with color desynchronization in Hass avocado

To find early (at harvest) biomarkers predictive of exocarp color desynchronization with softening, an integration of color-pigment, metabolite, and hormone datasets was conducted using the DIABLO algorithm from the mixOmics package. A *s*PLS-DA with two components was built using the average representation space of all datasets (Fig. 2A). The "sparse" function allows us to select the minimum number of variables from each dataset required to discriminate among the three harvest periods (early, middle, and late). In total, 13 color-pigment variables, 13 metabolites, and 9 hormones were selected, successfully distinguishing the samples by harvest time. As illustrated in Fig. 2A, variate 1 clearly separates early and late harvest exocarp samples, with mid-harvest exocarp samples positioned in between. Concurrently, variate 2 enhances the separation of mid-harvest exocarp samples from the other two harvest dates.

To determine which variables had the most significant contribution to the separation of the conditions studied, a correlation loading plot was generated (Fig. 2B). As expected, at the RTE stage, both the percentage of synchronized fruit, evaluated using a hedonic color scale, and the anthocyanin content (%$Black\ Fruit_{RTE}$ and $Anthocyanins_{RTE}$, respectively) exhibited positive correlations with harvest stage. Consequently, late harvest exocarp samples displayed greater color

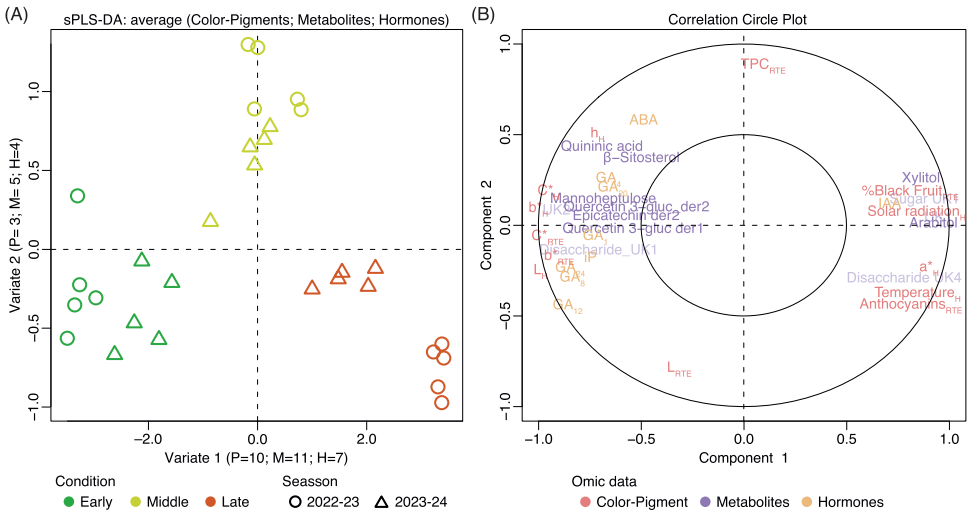

Fig. 2. Multi-omics integration reveals biomarkers of Hass avocado exocarp color – mesocarp firmness synchronization. (A) Sparse partial least squares discriminant analysis (*s*PLS-DA) was performed to discriminate early, middle, and late harvest exocarp samples, integrating color-pigment, metabolomic, and hormonal datasets. The analysis employed stringent variable selection to identify key biomarkers related to the desynchronization of exocarp color development and mesocarp softening. The number of selected variables contributing to each *s*PLS-DA component is specified on the respective axis. (B) sPLS-DA biplot depicting the correlation between selected variables and the corresponding avocado harvest stage, highlighting the specific contributions of each variable to the observed sample clustering.

synchronization with elevated anthocyanin levels. Furthermore, color parameters at RTE stage, measured using the CIELAB color scale, including the blue-yellow color (b^*_{RTE}), chroma (C^*_{RTE}), and lightness (L_{RTE}), were also highly correlated with harvest stage. Interestingly, even at harvest (when the fruits are still green and visual differences between early and late harvest exocarp samples are not observed), the CIELAB color measurement parameters (C^*_H, h_H, L_H, a^*_H, and b^*_H) showed strong correlation with early, middle, and late harvest exocarp

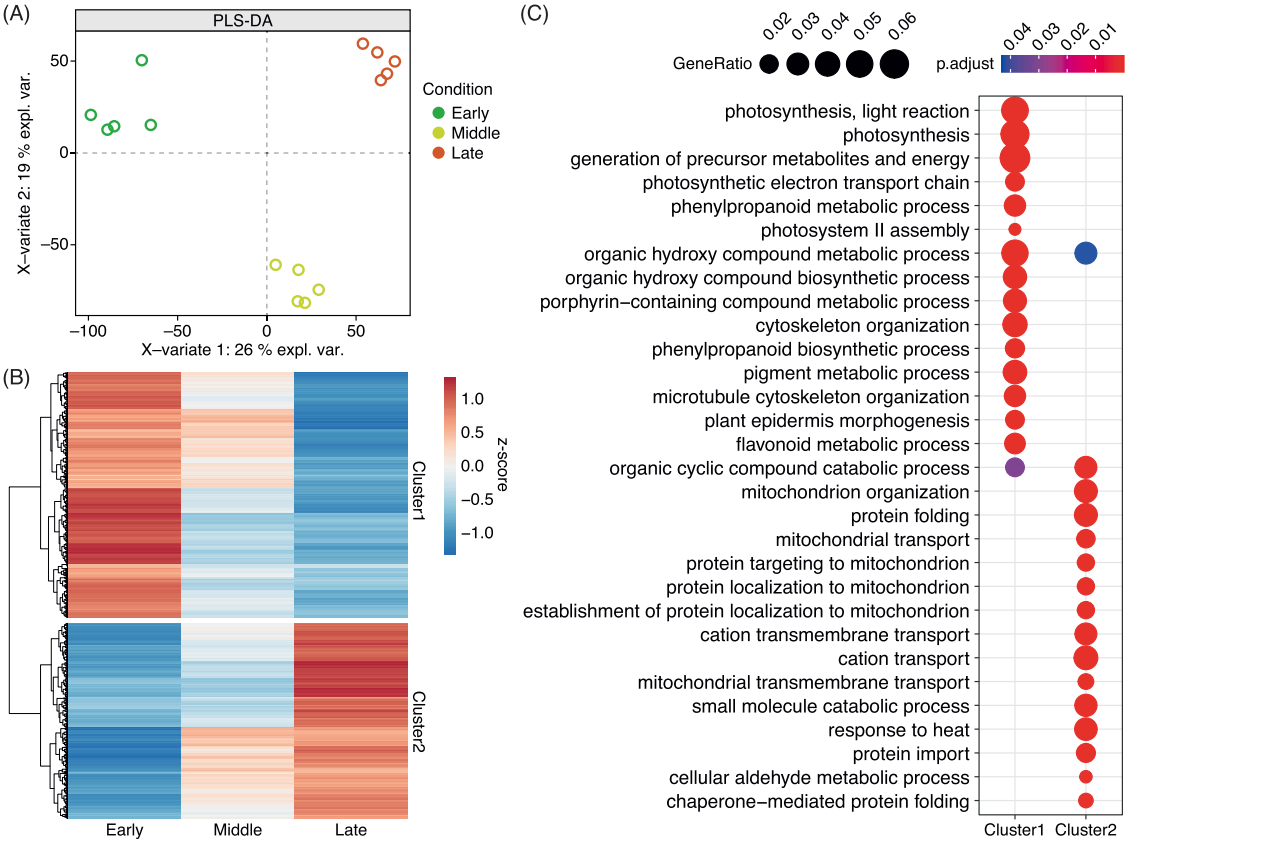

Fig. 3. Gene expression dynamics associated with avocado exocarp color- mesocarp softening desynchronization. (A) Partial least squares discriminant analysis (PLS-DA) of normalized gene expression data, illustrating replicate variability across a single harvest season (2022/2023). (B) Heatmap depicting monotonic differentially expressed genes (DEGs) between early, middle and late harvest stages. Expression values are z-score normalized and clustered based on decreasing or increasing expression patterns. (C) Gene ontology (GO) enrichment analysis of DEGs within clusters 1 and 2, highlighting functional categories related to color-softening desynchronization.

samples. These results suggest that CIELAB color measurement at harvest may serve as a valuable, non-destructive field tool for identifying fruit that is likely to exhibit color development problems.

Metabolic variables such as mannoheptulose, quercetin 3-glucoside derivatives, epicatechin derivatives, xylitol, and arabitol, as well as the hormone contents of ABA, gibberellins (GA_1, GA_4, GA_8, GA_{12}, GA_{20} and GA_{24}), iP, and IAA, were also identified as potential biomarkers of color desynchronization at harvest (unripen, green exocarp fruit). These variables show strong correlations with solar radiation and temperature at harvest (Solar $radiation_H$ and $Temperature_H$, respectively), which may be associated with an increased incidence of color desynchronization.

3.5. Transcriptomics analysis of the exocarp

Transcriptomic analyses of early, middle, and late harvest exocarp samples were performed in a single season, as shown in Fig. 3A. A PLS-DA model was constructed to evaluate sample distribution and replicate dispersion using normalized expression data. Consistent with previous results, early, middle, and late harvest samples could be separated along the x-variate 1, which accounted for 26 % of the explained variance.

The color-scaled heatmap in Fig. 3B displays the expression profiles of 3292 DEGs exhibiting a monotonic trend across harvest stages. Of these, 1832 DEGs with higher expression in early harvest samples were grouped into 'Cluster 1', while 1460 DEGs with elevated expression in late harvest samples were assigned to 'Cluster 2'. Both clusters showed a strong correlation with the incidence of the color desynchronization phenotype. A comparative GO enrichment analysis for Clusters 1 and 2 is shown in Fig. 3C. Cluster 1, enriched GO terms included photosynthesis and energy metabolism, cytoskeleton organization, and phenylpropanoid, flavonoid, and pigment biosynthetic pathways. In contrast, Cluster 2 was enriched for GO terms related to mitochondrial organization, protein and cation transport, and responses to heat stress.

3.6. Reconstruction of metabolic pathways involved in anthocyanin accumulation

The reconstruction of metabolic pathways involved integrating transcriptional, metabolic, and pigment data at harvest, revealing distinctions in several key biosynthetic routes. These included phenylpropanoid, flavonoid, and anthocyanin pathways (Fig. 4).

In the phenylpropanoid pathway, that contributes to the biosynthesis of lignin, which are essential structural polymers, early harvest samples showed high gene expression levels in 5 of 7 steps, while middle harvest samples presented high gene expression in 3. Coumaroyl-CoA also feeds into the flavonoid pathway, leading to the production of quercetin and epicatechin derivatives, as well as precursors for anthocyanin biosynthesis. Early harvest samples displayed both higher gene expression and elevated metabolite levels in this pathway, suggesting that as the fruit ripens, the activity of the flavonoid pathway increases resulting in increased production of these compounds. Finally, cyanidin enters the anthocyanin pathway, where genes such as UGT78D2 play a fundamental role in this stage, converting flavonoids into anthocyanins. This gene was overexpressed in late harvest samples concomitant with increased anthocyanin content at the RTE stage. Overall, these results indicate that early harvest fruit are still physiologically immature and have not fully developed the precursors associated with the anthocyanin synthesis pathway. As a result, they often fail to develop the expected color in the RTE stage.

4. Discussion

4.1. Orchard – specific differences and harvest maturity influenced exocarp color development at the ready to eat stage

Previous studies addressing this disorder have already reported the

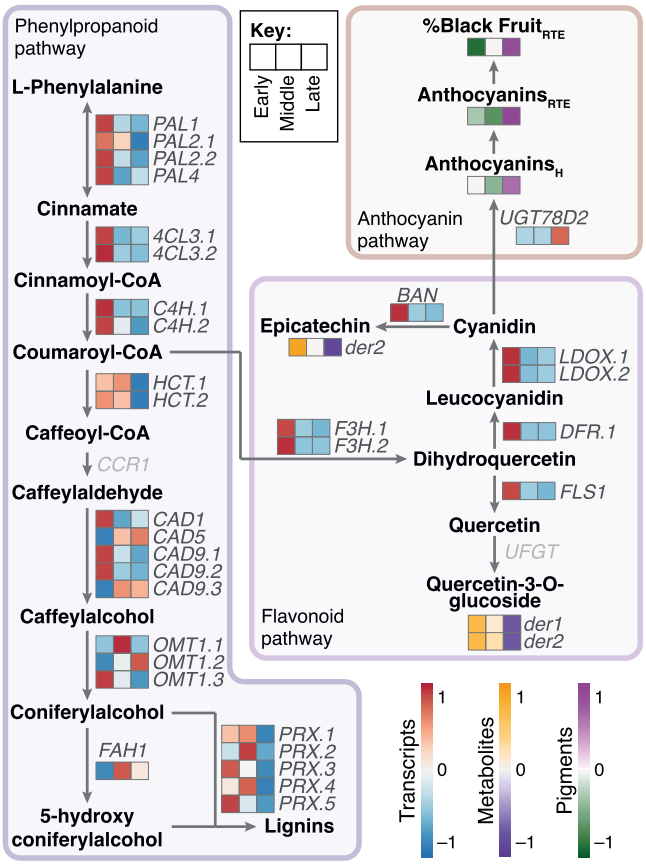

Fig. 4. Modeling of anthocyanin biosynthesis in avocado 'Hass' exocarp at different harvest times using metabolomic, transcriptomic and phenotypic data. All variables presented in this model, including those in the heatmap, exhibit differential expression/abundance with an FDR < 0.05. Grey gene/metabolite names represent no differential expression/abundance values between harvests. PAL: Phenylalanine ammonia lyase; 4CL: 4-Coumarate:CoA ligase; HCT: Hydroxycinnamoyl-CoA:shikimate hydroxycinnamoyl transferase; CCR: Cinnamoyl-CoA reductase; CAD: Cinnamyl-alcohol dehydrogenase; OMT: O-methyltransferase; FAH: Ferulic acid 5-hydroxylase; PRX: Peroxidase; BAN: BANYULS; F3H: Flavanone 3-hydroxylase; LDOX: Leucoanthocyanidin dioxygenase; DFR: Dihydroflavonol 4-reductase; FLS: Flavonol synthase; UFGT: UDP-glucose:flavonoid 3-O-glucosyltransferase; UGT78D2: UDP-glucosyl transferase 78D2.

marked effect of harvest maturity on exocarp color development, with early harvest fruit being more affected than late harvest fruit (Mathaba et al., 2015; Mathaba et al., 2016). In general, coastal orchards experience less extreme temperatures (11.3 °C mean temperature) compared to intermediate and interior zones (11.9 °C and 12.2 °C mean temperature, respectively) (Table S1), which may contribute to these differences. Previous studies have reported differences in the maturation pattern of avocados from the upper and lower parts of the orchard due to temperature variations (Mathaba et al., 2016; Mathaba et al., 2017). Arancibia-Guerra et al. (2022) observed this behavior in Chilean orchards located across different agroclimatic zones, noting that early harvest avocados (23 % - 26 % DM) developed a higher percentage of green fruit compared to middle harvest fruit (26 % - 30 % DM). On the other hand, studies examining 'Hass' avocado fruit with DM contents above 30 % have not reported issues with the development of the expected purple/black exocarp color (Olivares et al., 2024; Olmedo et al., 2024). These findings suggest that exocarp color development is strongly influenced by harvest maturity.

4.2. Phenotyping data reveals at harvest anthocyanin presence in late harvest unripen exocarp tissue

The differences in dry matter (DM) content ranges used to define harvest maturity across the two evaluated seasons likely reflect inter-seasonal climatic variability, which can influence oil accumulation and modify DM dynamics in Hass avocado fruit (Hernández et al., 2016). The observed decline in L*, a*, and b* color parameters suggests a progressive darkening of the exocarp, characterized by reduced brightness and diminished yellow hues, changes typically associated with ripening (Olivares et al., 2024). Notably, a* and hue angle (h) increased from harvest to the ready-to-eat (RTE) stage, indicating a shift along the red-green axis and supporting the hypothesis of chlorophyll degradation, which may unveil underlying anthocyanin pigmentation (Olmedo et al., 2024).

Previous studies have reported inconsistent trends in total chlorophyll and carotenoid concentrations in the exocarp of ripening 'Hass' avocado fruit, while total anthocyanin content tends to increase. For example, Arancibia-Guerra et al. (2022) found no significant differences in chlorophyll content between early and mid-harvest fruit. Similarly, Olivares et al. (2024) observed a decrease in chlorophyll content in fruit with > 30 % DM, from 301.1 mg kg^{-1} FW at harvest to 158.7 mg kg^{-1} FW at the RTE stage. These results align with the findings of Arancibia-Guerra et al. (2022), who also reported no significant changes in total chlorophyll or carotenoids across different harvest dates and maturity stages. In late-harvest fruit (>30 % DM), Ashton et al. (2006) documented a decrease in total chlorophyll from 170 to 120 μg g^{-1} FW and in carotenoids from 50 to 25 μg g^{-1} FW from harvest to the RTE stage.

It has been proposed that the degradation of chlorophylls and carotenoids during ripening allows anthocyanins to become more visually prominent in the exocarp (Cox et al., 2004). However, Arancibia-Guerra et al. (2022) suggested that the persistence of these pigments throughout ripening may be obscured by accumulating anthocyanins.

Classically, anthocyanin biosynthesis in 'Hass' avocado has been described as a postharvest event, coinciding with the initiation of ripening and accompanied by a marked skin color transition from green to black with purplish hues (Cox et al., 2004; Ashton et al., 2006). Nonetheless, the detection of anthocyanins at harvest in late-harvest, unripe fruit in the present study indicates that anthocyanin biosynthesis may begin preharvest, while the fruit is still attached to the tree. This observation diverges from previous reports by Arancibia-Guerra et al. (2022), Olivares et al. (2024), and Olmedo et al. (2024), in which anthocyanins were only detected at the RTE stage, even in fruit with elevated DM content (>30 %). Importantly, the significantly higher anthocyanin concentrations observed at the RTE stage in our study are consistent with findings by Arancibia-Guerra et al. (2022), who also reported greater anthocyanin accumulation in fruit harvested at more advanced harvest maturity.

4.3. Key metabolites and hormone profiles at harvest reveal transitions from growth and development towards physiological maturity and ripening initiation

The metabolites identified at different harvest maturities reflect a clear metabolic transition from active growth and development in early-harvest fruit to physiological maturity and the onset of ripening processes in late-harvest fruit. For instance, mannoheptulose, a seven-carbon carbohydrate known to act as a ripening inhibitor while the fruit remains attached to the tree (Pedreschi et al., 2019), was found in higher concentrations in early-harvested, physiologically immature fruit (DM 18–23 %; Hernández et al., 2016). Similarly, Olmedo et al. (2024) observed higher mannoheptulose levels in late-harvest avocado exocarp at harvest (>30 % DM; 43.5 g kg^{-1} DM) compared to the ready-to-eat (RTE) stage (9.7 g kg^{-1} DM), suggesting its subsequent utilization as a respiratory substrate.

Epicatechin derivatives, phenolic compounds involved in various metabolic processes including lipoxygenase activity and pathogen resistance (Guetsky et al., 2005), were present at higher concentrations in early-harvest fruit. Phenolic compounds, in concert with antioxidant enzymes, mitigate oxidative stress, support plant development, and enhance responses to biotic and abiotic stresses (Gupta et al., 2018). Consistent with our findings, Fuentealba et al. (2022) reported higher phenolic contents in early harvest avocado exocarp, whereas Uarrota et al. (2020) documented declining epicatechin derivatives with advancing maturity. Quinic acid, previously identified in avocado exocarp by López-Cobo et al. (2016), also showed decreasing levels associated with advanced harvest stages, suggesting its potential as a maturity marker. Although Campos et al. (2020) found no significant changes in quinic acid content across harvest stages, Chirinos et al. (2021) reported a substantial reduction (68.2 %) from early to mid-harvest in avocado mesocarp, consistent with findings in other fruit species such as 'Royal Gala' apples (Favre et al., 2022). Conversely, late harvest avocado exocarp exhibited increased concentrations of carbohydrates associated with advanced ripening and cell wall degradation, including xylitol, arabitol, mannitol, and unidentified disaccharides (Hernández et al., 2021). Previous analyses comparing metabolite profiles in slow and fast ripening avocado mesocarp at harvest have similarly linked elevated carbohydrate levels to advanced physiological age (Pedreschi et al., 2014).

Hormone profiles revealed elevated concentrations of gibberellins (GAs), abscisic acid (ABA), jasmonic acid (JA), and cytokinins (CKs) in early-harvest fruit relative to mid- and late-harvest stages. These hormones generally correlate with growth and developmental processes, whereas ABA notably increases during ripening (Günther et al., 2025). High GAs concentrations at harvest have been negatively correlated with the onset of the climacteric phase in 'Hass' avocado, suggesting that GAs delay ethylene and ABA accumulation, both essential for anthocyanin synthesis and exocarp color development (Günther et al., 2025). Supporting this observation, Hernández et al. (2022) found increased GA_1 and GA_4 levels in less mature avocado mesocarp, indicating GAs' indirect role in color development regulation. Despite typically low ABA concentrations at harvest (Arancibia-Guerra et al., 2022; Núñez-Lillo et al., 2023), our study detected higher ABA levels in early-harvest exocarp, possibly reflecting an early hormonal signaling event. JA, known to modulate anthocyanin biosynthesis by interacting with the MBW (MYB–basic Helix-Loop-Helix–WD40) complex via JAZ (jasmonate ZIM-domain) proteins (An et al., 2016), was also elevated in early-harvest fruit, aligning with Núñez-Lillo et al. (2023), who linked higher JA levels to color-softening desynchronization.

Salicylic acid (SA) content, previously associated with advanced biological age and reduced color desynchronization incidence (Hernández et al., 2022; Arancibia-Guerra et al., 2022), presented a similar trend. Auxins, critical in ripening regulation (McAtee et al., 2013) and typically known to inhibit ripening-associated anthocyanin synthesis (Gu et al., 2019; Jia et al., 2017; Ji et al., 2015), showed contrasting dynamics. Hernández et al. (2022) documented higher IAA levels in avocado mesocarp of advanced biological maturity, while Olmedo et al. (2024) reported elevated IAA concentrations (26.3 ng g^{-1} DM) in late harvest fruit exhibiting appropriate exocarp coloration. Additionally, IAA accumulation under controlled atmosphere (CA) conditions has been linked to enhanced synchronization between color and mesocarp softening in 'Hass' avocado (Arancibia-Guerra et al., 2022), suggesting auxins' complex role in ripening modulation.

4.4. Transcriptomic analysis supports a developmental shift from growth and development to physiological maturity and ripening initiation

Few transcriptomic studies have directly addressed the relationship between maturity or physiological age at harvest and gene expression profiles in 'Hass' avocado fruit. Hernández et al. (2022) analyzed transcriptomic differences in avocado mesocarp tissues categorized by

physiological age (E_0). Their results indicated that fruit with lower E_0 values exhibited enhanced expression of genes linked to active growth processes, including auxin transport, gibberellin and brassinosteroid biosynthesis, flavonol synthesis, and cell wall remodeling. Consistent with these observations, our data suggest that early harvest avocado exocarp tissues are still actively engaged in growth, preparing the molecular foundation necessary for subsequent ripening processes, such as color development.

Similarly, Olivares et al. (2022) studied transcriptomic variations in 'Hass' avocado exocarp across maturity stages defined as low dry matter (LDM, 20–23 % DM) and high dry matter (HDM, >27 % DM), after treatment with 1-MCP. They reported enrichment of gene functions related to cell wall biogenesis, phenylpropanoid metabolism, and secondary metabolite synthesis, which are critical for exocarp color development and overall ripening characteristics. These processes correlated with ethylene-responsive pathways, showing higher activation levels in HDM compared to LDM fruits.

Comparable transcriptomic patterns have been observed in peach (*Prunus persica*) by Núñez-Lillo et al. (2022), who identified differential gene expression between early and late harvested 'OxN' peaches. Early harvest fruit showed enrichment in genes related to RNA modification and photosynthetic activity, while late harvest fruit exhibited higher expression of genes associated with cell growth and cell wall remodeling. These observations parallel our findings in avocado, supporting the conclusion that early harvest fruit remain predominantly in a growth phase, while late harvest fruit have transitioned to developmental maturity and initiate ripening processes, including pathways involved in exocarp pigmentation.

5. Conclusions

A multi-omics analysis integrating transcriptomic, hormonal, and metabolomic data identified early metabolic biomarkers associated with different harvest dates and the desynchronization between avocado fruit color development and softening. Gene enrichment analysis revealed activation of phenylpropanoid and anthocyanin biosynthesis pathways, with higher expression levels observed in early and late harvested samples, respectively. Specifically, the overexpression of flavonoid biosynthesis genes within the phenylpropanoid pathway in early harvested samples suggests that the metabolic precursors and enzymatic machinery necessary for exocarp color development are still actively forming. In contrast, in late harvested samples, these components appear fully synthesized, promoting anthocyanin accumulation and the subsequent development of the characteristic black color associated with the ready to eat stage. These findings underscore the critical role of harvest timing in achieving proper synchronization between exocarp coloration and mesocarp softening at the ready to eat stage.

Author statement

Given her role as Associate Editor in the Journal Postharvest Biology & Technology, Romina Pedreschi had no involvement in the peer review of this article and had no access to information regarding its peer review. Full responsibility for the editorial process for this article was delegated to another journal editor.

CRediT authorship contribution statement

Excequel Ponce: Formal analysis, Data curation. **Romina Pedreschi:** Writing – review & editing, Supervision, Resources, Funding acquisition, Formal analysis, Conceptualization. **Ignacia Hernández:** Formal analysis, Data curation. **Claudio Meneses:** Writing – review & editing, Supervision, Resources, Methodology, Formal analysis. **Gerardo Núñez-Lillo:** Writing – original draft, Visualization, Software, Investigation, Data curation. **Reinaldo Campos-Vargas:** Writing – review & editing, Resources, Methodology, Formal analysis. **Camila Arancibia-Guerra:** Writing – original draft, Investigation, Formal analysis, Data curation. **David Campos:** Writing – review & editing, Resources, Methodology, Formal analysis. **Bruno Defilippi:** Writing – review & editing, Resources, Methodology, Formal analysis. **Jorge Baños:** Writing – review & editing, Resources, Methodology, Formal analysis. **Esther Carrera:** Writing – review & editing, Resources, Methodology, Formal analysis. **Lucía Olmo-García:** Writing – review & editing, Resources, Investigation, Formal analysis. **Alegría Carrasco-Pancorbo:** Writing – review & editing, Resources, Methodology, Formal analysis. **Nathalie Kuhn:** Writing – review & editing, Methodology, Formal analysis.

Declaration of Competing Interest

The authors declare that they have no known competing financial interests or personal relationships that could have appeared to influence the work reported in this paper. The author Romina Pedreschi is an Editorial Board Member/Associate Editor for this journal and was not involved in the editorial review or the decision to publish this article.

Acknowledgements

This study was financed by ANID-FONDECYT N°1220223, ANID – Millennium Science Initiative Program – ICN2021_044, and ANID-Vinculación Internacional-FOVI240006. Camila Arancibia-Guerra thanks ANID-Subdirección de Capital Humano/Doctorado Nacional/2022–21222076.

Appendix A. Supporting information

Supplementary data associated with this article can be found in the online version at doi:10.1016/j.postharvbio.2025.113787.

Data availability

Data will be made available on request.

References

An, J., Li, H., Song, L., Su, L., Liu, X., You, C., Wang, X., Hao, Y., 2016. The molecular cloning and functional characterization of MdMYC2, a bHLH transcription factor in apple. Plant Physiol Biochem. 108, 24–31. https://doi.org/10.1016/j.plaphy.2016.06.032.

Arancibia-Guerra, C., Núñez-Lillo, G., Cáceres-Mella, A., Carrera, E., Meneses, C., Kuhn, N., Pedreschi, R., 2022. Color desynchronization with softening of 'Hass' avocado: targeted pigment, hormone and gene expression analysis. Postharvest Biol. Technol. 194, 112067. https://doi.org/10.1016/j.postharvbio.2022.112067.

Ashton, O., Wong, M., McGhie, T., Vather, R., Wang, Y., Requejo-Jackman, C., Ramankutty, P., Woolf, A., 2006. Pigments in avocado tissue and oil. J. Agric. Food Chem. 54 (26), 10151–10158. https://doi.org/10.1021/jf061809j.

Campos, D., Teran-Hilares, F., Chirinos, R., Aguilar-Galvez, A., García-Ríos, D., Pacheco-Avalos, A., Pedreschi, R., 2020. Bioactive compounds and antioxidant activity from harvest to edible ripeness of avocado cv. Hass (*Persea americana*) throughout the harvest seasons. Int. J. Food Sci. Technol. 55, 2208–2218. https://doi.org/10.1111/ijfs.14474.

Chirinos, R., Campos, D., Martínez, S., Llanos, S., Betalleluz-Pallardel, I., García-Ríos, D., Pedreschi, R., 2021. The effect of hydrothermal treatment on metabolite composition of 'Hass' avocados stored in a controlled atmosphere. Plants 10 (11), 2427. https://doi.org/10.3390/plants10112427.

Cox, K., McGhie, T., White, A., Woolf, A., 2004. Skin colour and pigment changes during ripening of 'Hass' avocado fruit. Postharvest Biol. Technol. 31, 287–294. https://doi.org/10.1016/j.postharvbio.2003.09.008.

Dobd, M., Roehhr, J.T., Ahmed, R., Dieterich, C., 2012. Flexbar-flexible barcode and adapter processing for next-generation sequencing platforms. Biology 1 (3), 895–905. https://doi.org/10.3390/biology1030895.

Dobin, A., David, C.A., Schlesinger, G., Drenkow, J., Zaleski, C., Jha, S., Batut, P., Chaisson, M., Gingeras, T.R., 2013. STAR: ultrafast universal RNA-seq aligner. Bioinformatics 29, 15–21. https://doi.org/10.1093/bioinformatics/bts635.

Favre, L., Hunter, D.A., O'Donoghue, E.M., Erridge, Z.A., Napier, N.J., Somerfield, S.D., Hunt, M., McGhie, T.K., Cooney, J.M., Saei, A., Chen, R.K.Y., McKenzie, M.J., Brewster, D., Martin, H., Punter, M., Carr, B., Tattersall, A., Johnston, J.W., Gibon, Y., Heyes, J.A., Lill, R.E., Brummell, D.A., 2022. Integrated multi-omic analysis of fruit maturity identifies biomarkers with drastic abundance shifts

spanning the harvest period in 'Royal Gala' apple. Postharvest Biol. Technol. 193, 112059. https://doi.org/10.1016/j.postharvbio.2022.112059.
Ferreyra, R., Defilippi, B., 2012. Factores de pre-cosecha que afectan la post-cosecha de palta 'Hass', clima, suelo y manejos. Bol. INIA 248.
Fuentealba, C., Hernández, I., Saa, S., Toledo, L., Burdiles, P., Chirinos, R., Campos, D., Brown, P., Pedreschi, R., 2017. Colour and *in vitro* quality attributes of walnuts from different growing conditions correlated with key precursors of primary and secondary metabolism. Food Chem. 232, 664–672. https://doi.org/10.1016/j.foodchem.2017.04.029.
Fuentealba, C., Vidal, J., Zulueta, C., Ponce, E., Uarrota, V., Defilippi, B.G., Pedreschi, R., 2022. Controlled atmosphere storage alleviates Ħass´ avocado black spot disorder. Horticulturae 8, 369. https://doi.org/10.3390/horticulturae8050369.
Giusti, M.M., Wrolstad, R.E., 2001. Anthocyanins characterization and measurement with UV–visible spectroscopy. In: Wrolstad, R.E. (Ed.), Curr. Protoc. Food Anal. Chem. John Wiley & Sons, New York.
Gu, K.-D., Wang, C.-K., Hu, D.-G., Hao, Y.-J., 2019. How do anthocyanins paint our horticultural products? Sci. Hortic. 249, 257–262. https://doi.org/10.1016/j.scienta.2019.01.034.
Guetsky, R., Kobiler, I., Wang, X., Perlman, N., Gollop, N., Ávila-Quezada, G., Hadar, I., Prusky, D., 2005. Metabolism of flavonoid epicatechin by laccase of *Colletotrichum gloesporioides* and its effect on pathogenicity on avocado fruits. Phytopathology 95 (11), 1341–1348. https://doi.org/10.1094/PHYTO-95-1341.
Günther, C., Cooney, J., Billing, D., Jensen, D., Trower, T., Burdon, J., 2025. Gibberellin metabolism is important for modulating the pre-climacteric phase of 'Hass' avocado (Persea americana Mill.) fruit after harvest. Postharvest Biol. Technol. 222, 113365. https://doi.org/10.1016/j.postharvbio.2024.113365.
Gupta, D.K., Palma, J.M., Corpas, F.J., 2018. Antioxidant and antioxidant enzymes in higher plants, 1st ed. Springer International Publishing. https://doi.org/10.1007/978-3-319-75088-0. 978-3-3-75088-0.
Hatoum, D., Annaratone, C., Hertog, M.L., Geeraerd, A.H., Nicolai, B.M., 2014. Targeted metabolomics study of 'Braeburn' apples during long-term storage. Postharvest Biol. Technol. 96, 33–41. https://doi.org/10.1016/j.postharvbio.2014.05.004.
Hernández, I., Fuentealba, C., Olaeta, J.A., Lurie, S., Defilippi, B., Campos-Vargas, R., Pedreschi, R., 2016. Factors associated with postharvest ripening heterogeneity of Ħass´ avocado (*Persea americana* Mill.). Fruits 71, 259–268. https://doi.org/10.1051/fruits/2016016.
Hernández, I., Uarrota, V., Fuentealba, C., Paredes, D., Defilippi, B., Campos-Vargas, R., Nuñez, G., Carrera, E., Meneses, C., Hertog, M., Pedreschi, R., 2022. Transcriptome and hormone analyses reveals differences in physiological age of Ħass´ avocado fruit. Postharvest Biol. Technol. 185, 111806. https://doi.org/10.1016/j.postharvbio.2021.111806.
Hernández, I., Uarrota, V., Paredes, D., Fuentealba, C., Defilippi, B.G., Campos-Vargas, R., Meneses, C., Hertog, M., Pedreschi, R., 2021. Can metabolites at harvest be used as physiological markers for modelling the softening behavior of Chilean Ħass´ avocados destined to local and distant markets? Postharvest Biol. Technol. 174, 111457. https://doi.org/10.1016/j.postharvbio.2020.111457.
Ji, X.-H., Wang, Y.-T., Zhang, R., Wu, S.-J., An, M.-M., Li, M., Wang, C.-Z., Chen, X.-L., Zhang, Y.-M., Chen, X.-S., 2015. Effect of auxin, cytokinin and nitrogen on anthocyanin biosynthesis in callus cultures of red-fleshed apple (*Malus sieversii f. niedzwetzkyana*). Plant Cell Tiss. Organ Cult. 120, 325–337. https://doi.org/10.1007/s11240-014-0609-y.
Jia, H., Xie, Z., Wang, C., Shangguan, L., Qian, N., Cui, M., Liu, Z., Zheng, T., Wang, M., Fang, J., 2017. Abscisic acid, sucrose, and auxin coordinately regulate berry ripening process of the Fujiminori grape. Fuct. Integr. Genom. 17 (4), 441–457. https://doi.org/10.1007/s10142-017-0546-z.
Landahl, S., Terry, L.A., 2020. Non-destructive discrimination of avocado fruit ripeness using laser Doppler vibrometry. Biosyst. Eng. 194, 251–260. https://doi.org/10.1016/j.biosystemseng.2020.04.001.
Liao, Y., Smyth, G.K., Shi, W., 2019. The R package Rsubread is easier, faster, cheaper and better for alignment and quantification of RNA sequencing reads. Nucleic Acids Res. 47, 47. https://doi.org/10.1093/nar/gkz114.
Lichtenthaler, H.K., Buschmann, C., 2001. Chlorophylls and carotenoids: measurement and characterization by UV–VIS spectroscopy. Curr. Protoc. Food Anal. Chem. 1. F4.3.1-F4.3.8.
López-Cobo, A., Gómez-Caravaca, A.M., Pasini, F., Caboni, M.F., Segura-Carretero, A., Fernández-Gutierrez, A., 2016. HPLC-DAD-ESI-QTOF-MS and HPLC-FLD-MS as valuable tools for the determination of phenolic and other polar compounds in the edible part and by-products of avocado. LWT Food Sci. Technol. 505–513. https://doi.org/10.1016/j.lwt.2016.06.049.
Mathaba, N., Mafeo, T.P., Kruger, F.J., 2015. The skin colouring problema of 'Hass' avocado fruit during ripening. SAAGA Yearb. 38, 51–57.
Mathaba, N., Mathe, S., Mafeo, T.P., Tesfay, S.Z., Mlimi, J., 2017. Complexities of 'Hass' avocado skin colour change during ripening. SAAGA Yearb. 40, 129–132.
Mathaba, N., Mathe, S., Tesfay, S., Mafeo, T., Blakey, R., 2016. Effect of 1-MCP, production region, harvest time, orchard slope and fruit canopy position on Hass avocado colour development during ripening. SAAGA Yearb. 39, 100–105.
Mathe, S., Tesfay, S.Z., Mathaba, N., Blakey, R.J., 2018. Ripple effect of 1-methylcyclopropene on 'Hass' avocado colour development at different harvest times. Acta Hortic. (1201), 91–98. https://doi.org/10.17660/ActaHortic.2018.1201.13.
McAtee, P.A., Karim, S., Schaffer, R., David, K.M., 2013. A dynamic interplay between phytohormones is required for fruit development, maturation, and ripening. Front. Plant Sci. 4, 79. https://doi.org/10.3389/fpls.2013.00079.
Núñez-Lillo, G., Hernández, I., Olmedo, P., Ponce, E., Arancibia-Guerra, C., Sepulveda, L., Carrasco-Pancorbo, A., Beiro-Valenzuela, M., Carrera, E., Baños, J., Campos, D., Meneses, C., Pedreschi, R., 2024. Deciphering the behind blackspot exocarp disorder in avocado cv. Hass through a hormonal, transcriptional and metabolic integration approach. Postharvest Biol. Technol 218, 113163. https://doi.org/10.1016/j.postharvbio.2024.113163.
Núñez-Lillo, G., Perez-Reyes, W., Riveros, A., Lillo-Carmona, V., Rothkegel, K., Alvarez, J.M., Blanco-Herrera, F., Pedreschi, R., Campos-Vargas, R., Meneses, C., 2022. Transcriptome and gene regulatory network analyses reveal new transcription factors in mature fruit associated with harvest date in *Prunus persica*. Plants 11, 3473. https://doi.org/10.3390/plants11243473.
Núñez-Lillo, G., Ponce, E., Arancibia-Guerra, C., Carpentier, S., Carrasco-Pancorbo, A., Olmo-García, L., Chirinos, R., Campos, D., Campos-Vargas, R., Meneses, C., Pedreschi, R., 2023. A multiomics integrative analysis of color de-synchronization with softening of 'Hass' avocado fruit: A first insight into a complex physiological disorder. Food Chem. 408, 135215. https://doi.org/10.1016/j.foodchem.2022.135215.
Olivares, D., García-Rojas, M., Ulloa, P.A., Riveros, A., Pedreschi, R., Campos-Vargas, R., Meneses, C., Defilippi, B.G., 2022. Response mechanisms of 'Hass' avocado to sequential 1-methylcyclopropene applications at different maturity stages during cold storage. Plants 11, 1781. https://doi.org/10.3390/plants11131781.
Olivares, D., Ulloa, P.A., Vergara, C., Hernández, I., García-Rojas, M.A., Campos-Vargas, R., Pedreschi, R., Defilippi, B.G., 2024. Effects of delaying the storage of 'Hass' avocados under a controlled atmosphere on skin color, bioactive compounds and antioxidant capacity. Plants 13 (11), 1455. https://doi.org/10.3390/plants13111455.
Olmedo, P., Núñez-Lillo, G., Ponce, E., Alvaro, J.E., Baños, Carrera, E., González-Fernández, J.J., Hormaza, J.I., Campos, D., Chirinos, R., Campos-Vargas, R., Defilippi, B.G., Aguayo, E., Pedreschi, R., 2024. Metabolite profiling and hormone analysis of the synchronized exocarp-mesocarp development during ripening of cv. 'Fuerte' and 'Hass' avocado fruits. Food Biosci. 60, 104454. https://doi.org/10.1016/j.fbio.2024.104454.
Pedreschi, R., Muñoz, P., Robledo, P., Becerra, C., Defilippi, B., van Eekelen, H., Mumm, R., Westra, E., de Vos, R., 2014. Metabolomics analysis of postharvest ripening heterogeneity of Hass´ avocados. Postharvest Biol. Technol. 92, 172–179. https://doi.org/10.1016/j.postharvbio.2014.01.024.
Pedreschi, R., Uarrota, V., Fuentealba, C., Alvaro, J.E., Olmedo, P., Defilippi, B.G., Meneses, C., Campos-Vargas, R., 2019. Primary metabolism in avocado fruit. Front. Plant Sci. 10, 795. https://doi.org/10.3389/fpls.2019.00795.
Rivera, S.A., Ferreyra, R., Robledo, P., Selles, G., Arpaia, M.L., Saavedra, J., Defilippi, B. G., 2017. Identification of preharvest factors determining postharvest ripening behaviors in Ħass´ avocado under long term storage. Sci. Hortic. 2016, 29–37. https://doi.org/10.1016/j.scienta.2016.12.024.
Robinson, M.D., McCarthy, D.J., Smyth, G., 2010. EdgeR:a bioconductor package for differential expression analysis of digital gene expression data. Bioinformatics 26 (1), 139–140. https://doi.org/10.1093/bioinformatics/btp616.
Rohart, F., Gautier, B., Singh, A., Lé Cao, K.-A., 2017. MixOmics: an R package for 'omics feature selection and multiple data integration. PLoS Comput. Biol. 13 (11), e1005752. https://doi.org/10.1371/journal.pcbi.1005752.
Saavedra, J., Cordova, A., Navarro, R., Díaz-Calderón, P., Fuentealba, C., Astudillo-Castro, C., Toledo, L., Enrione, J., Galvez, L., 2017. Industrial avocado waste: functional compounds preservation by convective drying process. J. Food Eng. 198, 81–90. https://doi.org/10.1016/j.jfoodeng.2016.11.018.
Seo, M., Jikumaru, Y., Kamiya, Y., 2011. Profiling of hormones and related metabolites in seed dormancy and germination studies. Methods Mol. Biol. 773, 99–111. https://doi.org/10.1007/978-1-61779-231-1_7.
Singh, A., Shannon, C., Gautier, B., Rohart, F., Vacher, M., Tebbutt, S., Lê Cao, K., 2019. DIABLO: an integrative approach for identifying key molecular drivers from multi-omics assays. Bioinformatics 35, 3055–3062. https://doi.org/10.1093/bioinformatics/bty1054.
Uarrota, V.G., Hernández, I., Ponce, E., Vidal, J., Fuentealba, C., Defilippi, B.G., Lindh, V., Zulueta, C., Chirinos, R., Campos, D., Pedreschi, R., 2020. Unravelling factors associated with 'blackspot' disorder in stored Ħass´ avocado (*Persea americana* Mill.) fruit. J. Hortic. Sci. Biotech. 95 (6), 804–815. https://doi.org/10.1080/14620316.2020.1763860.
Yu, G., Wang, L.-G., Han, Y., He, Q.-Y., 2012. ClusterProfiler: an R package for comparing biological themes among gene cluster. OMICS, 16 (5), 284–287. https://doi.org/10.1089/omi.2011.0118.